

ICEMG 2023-XXXXX

a L-Type Modular Outer-Rotor Consequent-Pole Machine with Different Permanent Magnet and Iron Pole Sequences

Mohammadreza Naeimi¹, Karim Abbaszadeh², Johan Gyselinck³

¹K. N. Toosi University of Technology/Department of Electrical Engineering, Tehran; m.naeimi@kntu.email.ac.ir

²K. N. Toosi University of Technology/Department of Electrical Engineering, Tehran; abbaszadeh@kntu.ac.ir

³Université Libre de Bruxelles/ Department of Electro and Mechanical Systems, Brussels; johan.gyselinck@ulb.be

Abstract

Consequent-pole Permanent Magnet (CPM) machines have been widely proposed due to the high Permanent Magnet (PM) utilization ratio. However, CPM machines suffer from asymmetrical air gap flux density due to using PMs with the same polarity, which causes high torque ripple and asymmetrical back Electro Motive Force (EMF) voltage. So, the purpose of this paper is to present a new L-type modular outer-rotor consequent-pole permanent magnet (LMOCPM) machine with different PM and iron pole sequences to enhance the electromagnetic performance of CPMs. In order to reduce PM and rotor core volume simultaneously, the modular rotor is combined with the CPM concept to create a new structure for the PM machine. Consequently, rotor loss is low, and PM utilization is high in the proposed machine. Firstly, the different PM topologies with various N, S, and iron pole sequences are presented for the proposed LMOCPM machine. Then, LMOCPM machines and modular surface-mounted PM (MSPM) machine are investigated based on the magnetic circuit model to show the positive impacts of modular structures with unipolar PMs. A Finite Element Method (FEM) has also been used to analyze their electromagnetic performances, including air gap flux density, flux linkage, cogging torque, and on-load torque. Finally, the results show that the proposed LMOCPM machines use 39% less PM material than MSPM, although the average torque almost remains unchanged in LMOCPM1 and LMOCPM2 machines compared to the MSPM machine. As a result, the PM utilization ratio increased by 61%. Further, the torque ripple for the proposed LMOCPM1 and LMOCPM2 machines are dramatically dropped to 15.7% and 14.1%, whereas the MSPM machine torque ripple is 23.2%.

Keywords: Modular rotor, consequent-pole motor, iron pole, cogging torque, magnetic circuit model.

Introduction

The PM machines used rear-earth PM material as a magnetic potential source to achieve high torque and power density. However, the main challenge of the PM machines is the PM price for sensitive applications. Therefore, the switch reluctance machine [1], synchronous reluctance machine [2-3], hybrid PM machine [4], and hybrid rotor structure [5] are proposed in different research to reduce the PM volume for low-cost applications such as e-bike. Although the less or no-PM machines are developed in torque ripple and efficiency [6], they suffer from low power density and Power Factor (PF) [7].

The consequent pole method is a practical solution for PM volume saving in PM machines, which has been

extensively presented in [8-11]. The result of [8] showed that conventional CPM machines are able to achieve similar average torque while saving PM material approximately 20% with a dovetailed consequent-pole rotor. However, the CPM machine had more considerable core loss than conventional PM machines because of asymmetrical flux distribution. In [9], a new dual consequent-pole transverse flux motor is proposed that employs 16.5% less PM material than conventional SPMs and delivers 7.6% more torque density. However, the proposed motor still has a high cogging torque and low PF. In [10], the V-type consequent-pole permanent magnet machine is presented to reduce PM cost by removing half of the barriers and PMs. After removing PMs, the result showed that the PM volume decreased by 35% while the torque average fell from 12.5 Nm to 12.2 Nm. However, the torque ripple increased from 18% to 24.2%, and cogging torque doubled compared to conventional V-type PM machines. In [11], the axial flux rotor, which the PM placed between rotor teeth, was proposed and compared with a double-stator axial switched-flux PM machine. PM volume is dramatically saved by 50% in the proposed motor, even though both machines have a high torque ripple. Based on the results, the CPM topology is capable of improving PM utilization and reducing the PM material volume. Nevertheless, CPM has asymmetrical and unipolar Magnetic Motive Force (MMF) distribution of PMs, leading to asymmetrical and even-order harmonics of air gap flux density, asymmetrical phase back-EMF voltage, and an increase in torque ripple.

Different methods have been adopted to improve the performance of CPM in terms of electromagnetic and mechanical performance. In [12], a new staggered rotor structure is proposed for CPM to reduce the torque ripple by using PM with different polarities in different layers. The results demonstrated that it is possible to eliminate the even order harmonics in the phase back-EMF of a staggered rotor, despite the fact that it still produces a high torque ripple. Also, an innovative approach to improving the electromagnetic performance of CPM includes using modular structures. The modular stator structure reduces the flux path, resulting in less MMF requirement. As pointed out in [13], E-core modular CPM improved average torque without adding extra PM material. Furthermore, the C-core modular stator is a good candidate for reducing torque ripples. Authors in [14] employed an H-type modular stator to decouple the phase coupling flux, leading to improve fault tolerance. Further, modular spoke-type PM

machines are recommended in [15] and [16] for enhancing torque density and flux-weakening capabilities. However, PM utilization ratios in [15] were slightly diminished compared with conventional spoke type PM motors, and in [16], the structure of the motor led to significant even order harmonics.

As an update structure for the CPM machine, this paper proposes an L-type modular outer-rotor consequent-pole machine with different PM and iron pole sequences that offer significant performance improvements in torque ripple, average torque, and PM utilization ratio. The proposed machine not only reduces the PM and rotor core material volume by combining the modular rotor structure with the CPM concept, but also improves rotor loss and flux focusing. Firstly, the different sequences of PMs and iron poles are employed for the LMOCPM machine. Then, the working principles of LMOCPM and MSPM machines are presented by the simplified magnetic circuit model, and the flux magnet is investigated to derive the benefits of the L-type modular rotor structure. Moreover, the machines are analyzed based on FEM, and the electromagnetic performance of the LMOCPM machine, including air gap flux density, cogging torque, on-load torque, and flux linkage, is compared with the MSPM machine. Finally, the results illustrate that the proposed LMOCPM machines save 39.6% of PM volume compared to the MSPM machine with a high PM utilization ratio. Also, the torque ripple of LMOCPM1 and LMOCPM2 machines is reduced by 15.7% and 14.1%, although the MSPM machine has a 23.2% torque ripple.

Topology and Operating Principle of L-type Modular CP

The 36-slot and 32-pole configuration is employed for machines to analyze the electromagnetic performance of the MSPM machine and different PM arrangements of L-type modular CP. There are no differences between the machines in terms of rotor and stator dimension, stack length, number of windings turns, and air gap length for a fair comparison. The critical design parameters are detailed in "Table 1". Figure 1 (a) shows the MSPM machine, while Figure 1 (b) shows the LMOCPM machine (LMOCPM1). In this case, all PMs with S poles are removed, and the iron poles work as artificial S poles. It can be found from Figure 1 (c) that the LMOCPM machine is divided into two parts in LMOCPM2 which the placement of iron poles and magnets are switched in the second part, and the magnets have the opposite direction compared to the first part. So, the iron poles operate as virtual N poles in the second part of LMOCPM2. In LMOCPM3, the rotor is divided into four parts. The location of the iron and PM poles is periodically changed in each part. Also, the magnetic direction of magnets is reversed by changing the location of iron poles and PMs. However, the PMs in each part have the same magnetic direction, as shown in Figure 1 (d). A white arrow indicates the PM magnetization direction of each machine, as shown in Figure 1. It can be observed from the figures that all proposed machines have an L-type modular structure, and salient poles replace half of PMs. Each module includes an iron pole, a PM, and a rotor back iron, adding a flux barrier between rotor modules in the CP machine.

Table 1. General specifications of machines

Parameter	Value	Unit
Machine pole pairs	16	-
Number of stator teeth	36	-
Magnet thickness	3.5	mm
Stator outer diameter	80	mm
Rotor outer diameter	100	mm
Stack length	50	mm
Air gap length	0.5	mm
Rated current	2.5	A
Rated speed	187.5	RPM

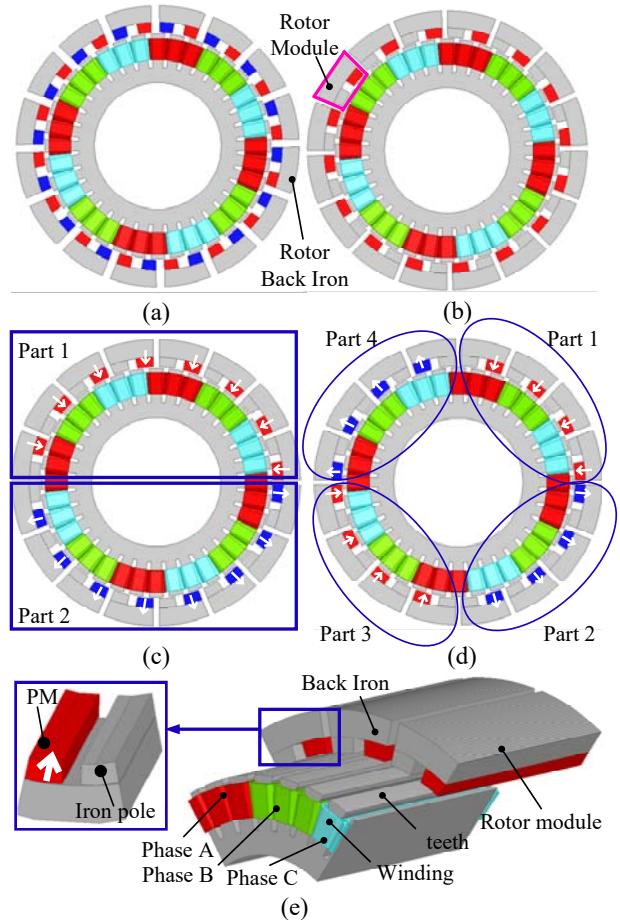


Figure 1. Cross-sections of four PM machines with different rotors. (a) modular surface-mounted PM (MSPM) motor, (b) L-type modular outer-rotor consequent-pole (LMOCPM1), (c) LMOCPM2, (d) LMOCPM3, (e) 3-D view of LMOCPM1

A simplified magnetic circuit model (MCM) for the MSPM machine and the proposed LMOCPM machine are respectively illustrated in Figure 2(a) and (b) to demonstrate the effect of the L-type modular consequent-pole machine on air gap flux. R_r , R_m , R_g , R_t , R_i , R_s , and R_{gb} are the rotor back iron, PM, air gap, teeth, iron pole, stator yoke and flux barrier reluctance, respectively. F_{PM} is the PM MMF. ϕ_{g1} and ϕ_{g2} of MSPM machine are the air gap flux under N and S poles, respectively. ϕ_{g1}'' and ϕ_{g2}'' of the proposed LMOCPM machine are the air gap flux under N and iron poles, respectively. It should be noted that the leakage flux between PMs, PM and iron poles, and slots neglect to simplify the machine model.

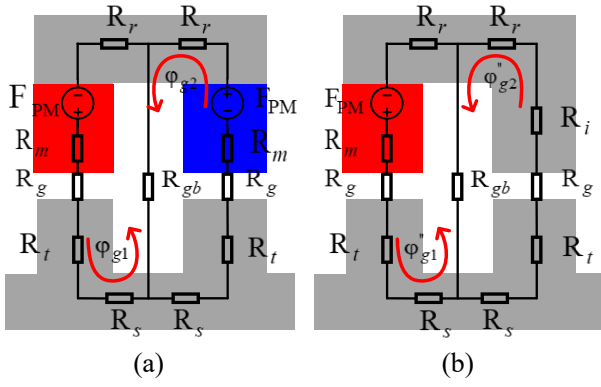


Figure 2. magnetic circuit model of (a) MSPM machine and (b) proposed LMOCPM machine

For the proposed LMOCPM and MSPM machines, Kirchhoff's laws for MCM provide the following magnetic equations as

$$(R_s + R_r + R_g + R_t + R_m)\phi_{g1} + R_{gb}(\phi_{g1} - \phi_{g2}) = F_{PM} \quad (1)$$

$$(R_s + R_r + R_g + R_t + R_m)\phi_{g2} + R_{gb}(\phi_{g2} - \phi_{g1}) = F_{PM} \quad (2)$$

$$(R_s + R_r + R_g + R_t + R_m)\phi_{g1}'' + R_{gb}(\phi_{g1}'' - \phi_{g2}'') = F_{PM} \quad (3)$$

$$(R_s + R_r + R_g + R_t + R_i)\phi_{g1}'' + R_{gb}(\phi_{g2}'' - \phi_{g1}'') = 0 \quad (4)$$

where the reluctance for the path of the PM pole and the iron pole are respectively defined as

$$R_T = R_s + R_r + R_g + R_t + R_m \quad (5)$$

$$R_{CT} = R_s + R_r + R_g + R_t + R_i \quad (6)$$

In matrix format, equations (1)-(4) can be rewritten as following

$$\begin{bmatrix} R_T + R_{gb} & -R_{gb} \\ -R_{gb} & R_T + R_{gb} \end{bmatrix} \begin{bmatrix} \phi_{g1} \\ \phi_{g2} \end{bmatrix} = \begin{bmatrix} F_{PM} \\ F_{PM} \end{bmatrix} \quad (7)$$

$$\begin{bmatrix} R_T + R_{gb} & -R_{gb} \\ -R_{gb} & R_{CT} + R_{gb} \end{bmatrix} \begin{bmatrix} \phi_{g1}'' \\ \phi_{g2}'' \end{bmatrix} = \begin{bmatrix} F_{PM} \\ 0 \end{bmatrix} \quad (8)$$

by solving (7)-(8), the magnetic fluxes for PM poles (ϕ_{g1}'' , ϕ_{g2}'') and iron poles path (ϕ_{g1} , ϕ_{g2}) of the proposed LMOCPM and MSPM machines can be obtained as

$$\phi_{g1} = \phi_{g2} = \frac{F_{PM}}{R_T} \quad (9)$$

$$\phi_{g1}'' = \frac{(R_{CT} + R_{gb})F_{PM}}{(R_T + R_{gb})(R_{CT} + R_{gb}) - R_{gb}^2} \quad (10)$$

$$\phi_{g2}'' = \frac{R_{gb} \times F_{PM}}{(R_T + R_{gb})(R_{CT} + R_{gb}) - R_{gb}^2} \quad (11)$$

It can be observed from equation (9) that the flux magnet of the MSPM machine under the N and S poles is equal in each module. However, the air gap flux density and flux magnet of the conventional CPM machine has an asymmetrical shape due to the unipolar PMs. Consequently, even order harmonics of air gap flux

density cause high torque ripples and asymmetrical phase back-EMF voltage. According to equations (10)-(11), the LMOCPM machine has a different magnet flux under PM and iron poles due to substituting all S poles with iron poles. But the flux magnet and air gap flux density are more symmetrical than conventional CPM by employing an L-type modular rotor. The reluctances of iron parts such as stators, rotors, and iron poles are neglectable because of the high permeability compared to the air gap reluctance. So, the proportion of flux magnet under PM poles and iron poles for the proposed machine can be defined as

$$\frac{\phi_{g1}''}{\phi_{g2}''} = \frac{R_{gb} + R_g}{R_{gb}} \quad (12)$$

It can be perceived from equation (12) that the flux magnet under PM and iron poles can be approximately equal in proposed LMOCPM machine if R_{gb} is sufficiently greater than R_g . Also, the proposed LMOCPM1, LMOCPM2, and LMOCPM3 machines exhibit more air gap flux density harmonics owing to unipolar PM MMF distributions, double slot structure, and modular rotor structure, which results in more harmonics engaged in torque production.

Performance Analysis

Air gap Flux Density and Flux Magnet

To illustrate the improvement effect of the L-type modular structure and different PM topologies, Figures 3 and 4 respectively show the open-circuit flux density waveform and flux linkage in MSPM, LMOCPM1, LMOCPM2, and LMOCPM3 motors. It can be seen that the MSPM machine has a 1.8T peak-to-peak air gap flux density because of the more PM MMF sources (high PM volume in structure), although the proposed LMOCPM1 and LMOCPM2 motors have a 1.65T peak-to-peak. Also, the lowest peak value of air gap flux density belongs to the LMOCPM3 motor due to including both PMs polarity and high flux leakage. Figure 4 shows the difference between the L-type modular structure and the L-type modular consequent-pole structure is neglectable in the phase flux linkage, although the PM volume is reduced by 39.6% in LMOCPM1, LMOCPM2, and LMOCPM3 motors.

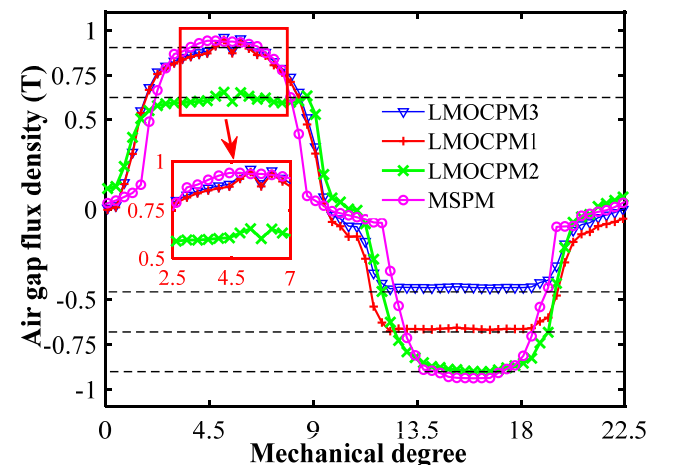


Figure 3. Open circuit air gap flux density waveform of proposed machines

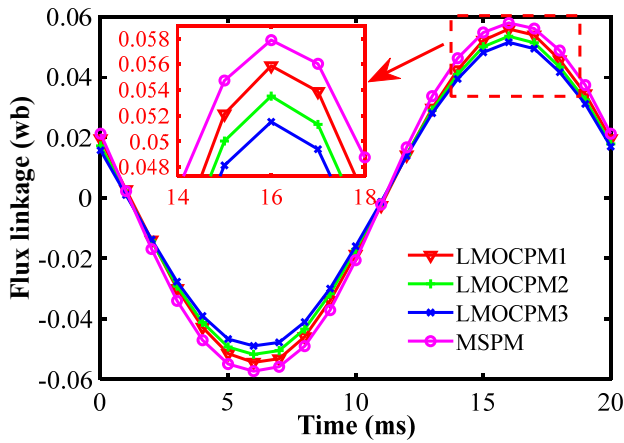


Figure 4. Flux linkage waveform of proposed machines

Therefore, the LMOCPM1 and LMOCPM2 machines have more symmetrical air gap flux density than the LMOCPM3 machine compared to the MSPM machine. The results validate the MCM analysis that the L-type modular structure can provide a symmetrical air gap flux density when PMs share the same magnetization direction. The details effect of the proposed L-type modular structure on air gap flux density and flux magnet will be thoroughly analyzed in future work.

Torque and Torque Ripple

The electromagnetic torque waveforms of the proposed machines are illustrated in Fig. 5. It can be observed that the MSPM machine produce the highest average torque among the L-type modular structure because it contains the most PM volume. In contrast, the MSPM machine has a lower PM utilization ratio in comparison with the LMOCPM1, LMOCPM2, and LMOCPM3 machines. LMOCPM1 and LMOCPM2 machines have 39.6% less PM volume with almost the same average torque, which is 2.05N.m and 1.94N.m, respectively. Although the PM volume is reduced from 26.8cm³ to 16.2cm³ in LMOCPM1, LMOCPM2, and LMOCPM3 machines compared to the MSPM machine, the average torque changes slightly. The reason is that the proposed machines exploit a double slot structure and PM with the same polarity, resulting in engaging more harmonic in torque generation.

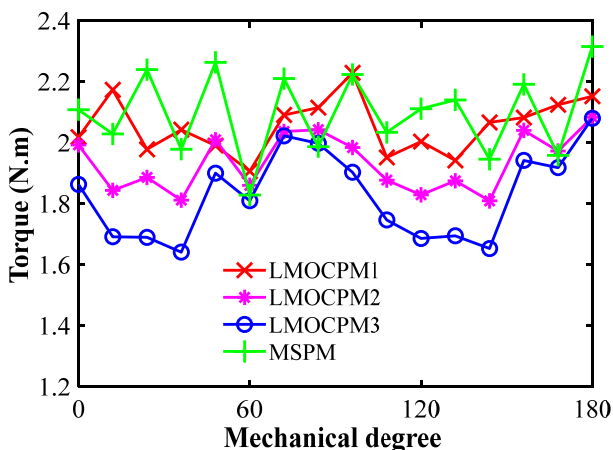


Figure 5. Torque waveform with rotor position for proposed machines

Meanwhile, it can be seen in Figure 5 that the LMOCPM2 and LMOCPM3 machines have the lowest and highest torque ripple among machines which is 14.1% and 24%, respectively. Moreover, the torque ripples of LMOCPM1 and MSPM machines are 15.7% and 23.2%. So, the proposed L-type modular consequent pole has the capability to suppress the disruptive torque harmonics along with reducing the PM volume.

Cogging Torque

The proposed machines have different peak-to-peak values for cogging torque due to employing different PM and iron pole sequences while adopting the same dimension for the rotor and stator. Figure 5 are shown the cogging torques of four machines. It can be seen that peak-to-peak cogging torques of LMOCPM2 and LMOCPM3 machines are dramatically decreased by 134mN.m and 151mN.m, respectively. However, the MSPM has the highest peak-to-peak value, which is 428mN.m. The reason is that the PMs polarity and iron poles and PMs placement are periodically reversed and changed with each other in LMOCPM2 and LMOCPM3 machines, which results in including both PMs polarity as well less PM volume.

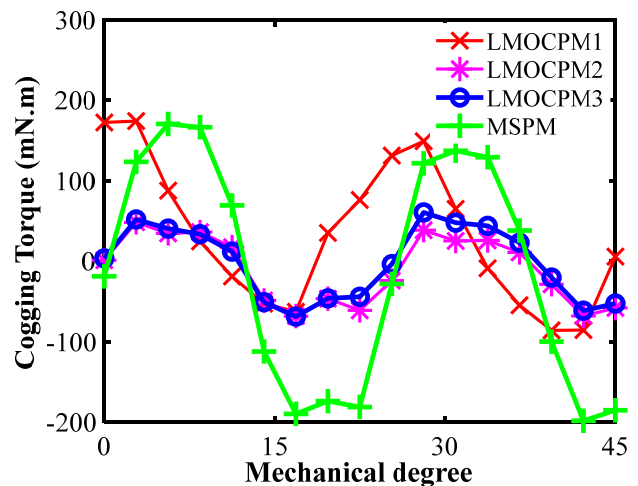


Figure 6. Cogging torque waveform of proposed machines

Conclusions

This paper proposed the new L-type modular outer-rotor consequent-pole machine to achieve high PM utilization and low torque ripple simultaneously. In order to conduct a comprehensive investigation, The PMs of the proposed LMOCPM machine with N-iron arrangement was divided into two and four groups for LMOCPM2 and LMOCPM3 machines to change the PM polarity of each group periodically. Then the topology was presented based on MCM, and FEM was employed to illustrate electromagnetic performance, including air gap flux density, torque waveform, cogging torque, and flux linkage. The LMOCPM1, LMOCPM2, LMOCPM3, and MSPM machines were compared to demonstrate the effect of different PM and iron pole arrangements, the modular structure, and PM with the same polarity. The results showed that the proposed LMOCPM machines are cost-effective

compared to the MSPM machine, saving 39.6% PM volume. Besides, the average torques of LMOCPM1 and LMOCPM2 machines almost remained unchanged compared to MSPM machines when the torque ripples were decreased by 15.7% and 14.1%, respectively. Also, the LMOCPM2 machine has the lowest cogging torque among the proposed machines. Thus, the LMOCPM2 machine is an applicable candidate for applications where low torque ripple, high torque density generation capability, and high PM utilization ratio are preliminary requirements.

References

- [1] Howey, B., Bilgin, B., and Emadi, A., 2020. "Design of an External-Rotor Direct Drive E-Bike Switched Reluctance Motor". *IEEE Transactions on Vehicular Technology*, 3(69), March, pp. 2552-2562.
- [2] Naeimi, M., Nasiri-Zarandi, R., and Abbaszadeh, K., 2021. "C & Circular Shaped Barriers Optimization in a Synchronous Reluctance Rotor for Torque Ripples Minimization". *Scientia Iranica*.
- [3] Naeimi, M., Abbaszadeh, K., and Nasiri-Zarandi, R., 2021. "Torque ripples reduction in a synchronous reluctance motor by rotor parameters optimization". *COMPEL - The international journal for computation and mathematics in electrical and electronic engineering*, 6(40), pp. 1053-1066, 2021.
- [4] Qiao, G., Liu, Y., Wang, M., Liu, F., and Zheng, P., 2022. "Study of a High-Efficiency Series-Parallel-Connected Hybrid-PM Variable-Flux Permanent Magnet Synchronous Machine". *IEEE Transactions on Magnetics*, 2(58), Feb., pp. 1-7.
- [5] Shen, J. -X., Lin, Y. -Q., Sun, Y., Qin, X. -F., Wan, W. -J., and Cai, S., 2022. "Permanent Magnet Synchronous Reluctance Machines with Axially Combined Rotor Structure". *IEEE Transactions on Magnetics*, 2(58), Feb., pp. 1-10.
- [6] Lin, J., Schofield, N., and Emadi, A., 2015. "External-Rotor 6–10 Switched Reluctance Motor for an Electric Bicycle". *IEEE Transactions on Transportation Electrification*, 4(1), Dec., pp. 348-356.
- [7] Credo, A., Fabri, G., Villani, M., and Popescu, M., 202. "Adopting the Topology Optimization in the Design of High-Speed Synchronous Reluctance Motors for Electric Vehicles". *IEEE Transactions on Industry Applications*, 5(56), Sept.-Oct., pp. 5429-5438.
- [8] Li, J., Wang, K., and Liu, C., 2018. "Torque Improvement and Cost Reduction of Permanent Magnet Machines with a Dovetailed Consequent-Pole Rotor". *IEEE Transactions on Energy Conversion*, 4(33), Dec., pp. 1628-1640.
- [9] Yang, X., Kou, B., Luo, J., and Zhang, H., 2021. "A Novel Dual-Consequent-Pole Transverse Flux Motor and Its Analytical Modeling". *IEEE Transactions on Industrial Electronics*, 5(68), May, pp. 4141-4152.
- [10] Kwon, J. -W., Li, M., and Kwon, B. -I., 2021. "Design of V-Type Consequent-Pole IPM Machine for PM Cost Reduction with Analytical Method". *IEEE Access*, (9), pp. 77386-77397.
- [11] Zhao, J., Quan, X., Sun, X., Li, J., and Lin, M., 2020. "Design of a Novel Axial Flux Rotor Consequent-Pole Permanent Magnet Machine". *IEEE Transactions on Applied Superconductivity*, 4(30), June, pp. 1-6.
- [12] Li, J., Wang, K., and Li, F., 2019. "Reduction of Torque Ripple in Consequent-Pole Permanent Magnet Machines Using Staggered Rotor". *IEEE Transactions on Energy Conversion*, 2(34), June, pp. 643-651.
- [13] Li, G. J., Zhu, Z. Q., Chu, W. Q., Foster, M. P., and Stone, D. A., 2014. "Influence of flux gaps on electromagnetic performance of novel modular PM machines". *IEEE Trans. Energy Convers.*, (29), April, pp. 716-726.
- [14] Ullah, W., and Khan, F., 2021. "Design and Performance Analysis of a Novel Outer-Rotor Consequent Pole Permanent Magnet Machine With H-Type Modular Stator". *IEEE Access*, (9), pp. 125331-125341.
- [15] Li, J., and Wang, K., 2019. "A Novel Spoke-Type PM Machine Employing Asymmetric Modular Consequent-Pole Rotor". *IEEE/ASME Transactions on Mechatronics*, 5(24), Oct., pp. 2182-2192.
- [16] Zhang, H., Hua, W., Wu, Z., and Zhu, X., 2018. "Design Considerations of Novel Modular-Spoke-Type Permanent Magnet Machines". *IEEE Transactions on Industry Applications*, 5(54), Sept.-Oct., pp. 4236-4245.